Soft Matter

Accepted Manuscript

ROYAL SOCIETY OF CHEMISTRY

www.rsc.org/softmatter

Supercoiling Transformation of Chemical Gels

Makoto Asai[1*]

Chemical Engineering, Columbia University, 500 W 120th St., New York, NY 10027, USA

Takuya Katashima

Department of Macromolecular Science, Osaka University,

1-1, Machikaneyama-cho, Toyonaka, Osaka, 560-0043, Japan

Takamasa Sakai[*]

Department of Bioengineering, School of Engineering, The University of Tokyo,

7-3-1 Hongo, Bunkyo-ku, Tokyo 113-8656, Japan

Mitsuhiro Shibayama[*]

Institute for Solid State Physics, The University of Tokyo, 5-1-5, Kashiwanoha,

Kashiwa, Chiba, 277-8581, Japan

Corresponding Authors

Correspondence should be addressed to M. A. (email: ma3284@columbia.edu) or T. S. (email: sakai@tetrapod.t.u-tokyo.ac.jp) or M. S. (email: sibayama@issp.u-tokyo.ac.jp)

Abstract

The swelling/deswelling behavior of chemical gels has been an unsolved problem disputed over for a long time. The Obukhov-Rubinstein-Colby model depicts the influence that swelling/deswelling has on elasticity, but its physical picture is too complicated to be sufficiently validated by experiment. In this study, we use molecular dynamics simulation to verify the validity of the molecular picture of network strands predicted by the Obukhov-Rubinstein-Colby model. We conclude that the physical picture of the Obukhov-Rubinstein-Colby model is reasonable, and furthermore the simulation can reveal details of conformational changes in network strands during the supercoiling transformation. Our findings do not only reveal the validity, but also give a better understanding of the dynamics of the swelling/deswelling behavior of chemical gels.

Table of Content

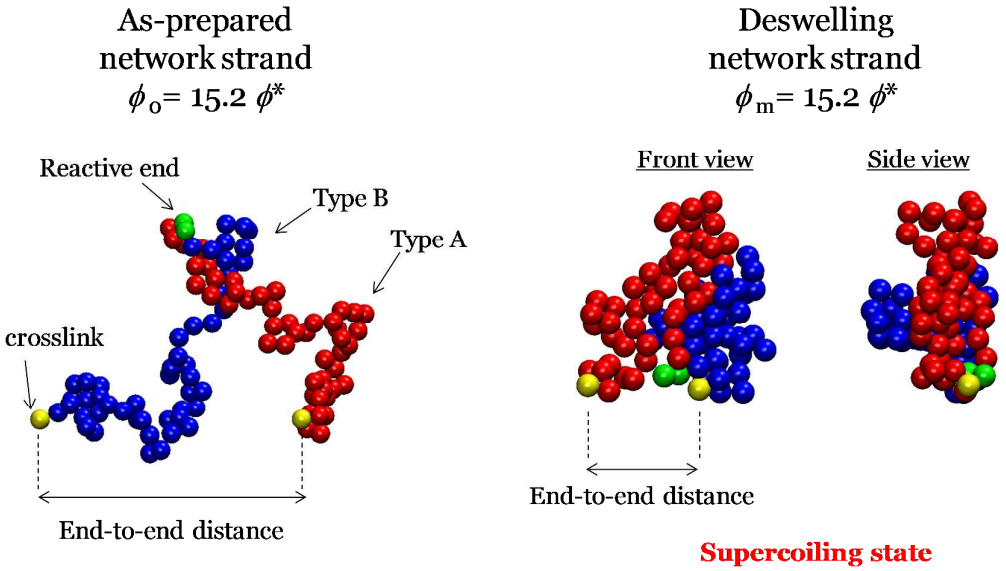

Introduction

Polymer gels contain solvents within the three-dimensional polymer network. It is commonly known that the mechanical properties of polymer gels strongly depend on polymer concentrations at prepared state (ϕ_0) and at the measured state after swelling/deswelling (ϕ_m). There have been many experimental and theoretical studies of these relationships.[1-21] Originally, Flory *et al.* treated this problem theoretically[4, 22] and assumed that crosslinks move affinely due to the swelling and deswelling and that the network strands take a random coil conformation in all concentration regions. Under these assumptions, they predicted the elastic modulus of polymer gels as a function of ϕ_0, ϕ_m and the degree of polymerization of the network strands (N). Obukhov *et al.* modified Flory's rubber theory by taking into account the excluded volume effect on the fractal dimension of network strands (Obukhov-Rubinstein-Colby model).[8] Obukhov *et al.* showed that the ϕ_0-, ϕ_m-dependences of the elastic modulus are strongly influenced by the excluded volume effect, and these dependences depend on the concentration regimes of

ϕ_0 and ϕ_m. Furthermore, they predicted abnormal mechanical properties for strongly deswollen networks. When gels are strongly deswollen from the preparation state ($\phi_m >> \phi_0$), network strands are expected to have a more compact conformation than the random coil due to a reduction in gel volume, which is called supercoiling. They also predicted that the supercoiling of network strands has significant effects not only on the elastic modulus but also on large deformation behavior. The details of this model are described in *Theoretical Background.*

The Obukhov-Rubinstein-Colby model has been examined by several experimental studies. Urayama *et al.* showed that the equilibrium swelling ratio is influenced not only by ϕ_0 but also by the quality of solvent. [14] Reference 16 demonstrates that these exists a crossover in the ϕ_m-dependence of the elastic modulus around the concentration where the excluded volume effect is fully screened (ϕ^{**}). References 17 and 18 also demonstrate that fully deswollen networks prepared at low ϕ_0 exhibit remarkable extensibility as well as unusually weak strain dependence of tensile stress and argue that these

features result from the strongly collapsed conformation of network strands.

In our previous studies, we employed the Tetra-arms-Polyethylene Glycol gels (Tetra-PEG gels) as a model system to investigate the validity of the Obukhov-Rubinstein-Colby model experimentally.[12, 21] The Tetra-PEG gel is formed by AB type cross-link-coupling, where there are two types of tetra-PEG in the system whose reactive ends only react with those of the opposite type. (See Figure 1). [23] Here, a Tetra-PEG itself can be regarded as a cross linker, so we call this reaction "cross-link-coupling". According to previous experimental and simulation studies, Tetra-PEG gel has a high reaction conversion, few elastically ineffective loops, and few trapped entanglements, which corresponds to an ideal or near-ideal network. [23-32] In reference 12 and 21, we demonstrated crossovers in the ϕ_m-dependence of the elastic modulus at approximately the overlapping concentration (ϕ^*) and at the concentration where the elastic contribution of entangled chains become dominant. Furthermore, using the Pincus blob concept, [33] we suggested that the radius of gyration decreases with increasing ϕ_m in the supercoiling region. These

experimental results support the Obukhov-Rubinstein-Colby model prediction.

Although theoretical predictions are well supported by experimental results, the direct verification of the theoretical assumptions is still difficult because of experimental inaccessibility to the molecular level. For example, the conformation of network strands and the topological relationship between strands cannot be directly observed. Recently, molecular dynamics (MD) simulation has been widely applied in many different fields, and has provided information about microscopic pictures of network structure. [26, 31, 34-48] In the present study we use MD simulations to reproduce the swelling/deswelling of a polymer network after preparation. We have already reported that our MD simulation can produce realistic network structure for Tetra-PEG gels. [31] In this paper we discuss the following: (1) investigation of the conformation of the network strand in its swollen and deswollen states; (2) verification of the Obukhov-Rubinstein-Colby model; (3) the affine deformation of crosslinks and the change in the fractal dimension of network strands.

Theoretical background

We describe here the theoretical background for the relationships between the elastic modulus and the polymer volume fraction for gels in their swollen and deswollen states, roughly following reference 8. The Obukhov-Rubinstein-Colby model is based on Flory-Rehner's assumption that the elastic part of free energy (F_{el}) and the mixing part of free energy (F_{mix}) are separable. [4, 5]

The elastic free energy, F_{el} is given by

$$\frac{F_{\mathrm{el}}}{a^3} \cong \frac{E}{3} = \nu_{\mathrm{el}} F_{\mathrm{el}}^0 = \frac{\phi}{a^3 N} F_{\mathrm{el}}^0 \qquad (1)$$

Where a^3 is the volume of a monomer, E is the elastic modulus, ν_{el} is the number of elements contributing to elasticity, and F_{el}^0 is the elastic energy of a single element. The Obukhov-Rubinstein-Colby model adapts the physical picture suggested by Panyukov, [49] which describes the elastic part of free energy F_{el}^0 as $k_{\mathrm{B}}T$ per strand times the Gaussian perturbation from the chains' preferred state at that concentration;

$$F_{\mathrm{el}}^{0} \cong \left(\frac{\lambda R_0}{R_{\mathrm{ref}}}\right)^2 k_{\mathrm{B}}T \qquad (2)$$

Here, R_0 is the root-mean-square end-to-end distance of network strands in their ϕ_0 with degree of polymerization N. $\lambda(\equiv(\phi_0/\phi_{\mathrm{m}})^{1/3})$ is uniaxial expansion of an elastic strand. R_{ref} is the end-to-end distance of a free chain with degree of polymerization N, when the concentration is the same as that of the polymer network at ϕ_{m}. The Obukhov-Rubinstein-Colby model assumes that swelling causes network junctions to move affinely. On average, junctions move apart on swelling by the same linear expansion λ as macroscopic network. According to Eq. (2), elastic part of free energy is affected by ϕ_0 and ϕ_{m}. In a dilute system with good solvent, R is ϕ-independent and represented as [3]

$$R \cong bN^{\nu} \qquad (\phi_0 < \phi^*), \qquad (3)$$

Here, b is the root-mean-square average bond length, ϕ^* is the polymer volume fraction at the onset of the overlapping of the star polymer chains, and ν is the exponent of the excluded volume effect. The exponent is $\nu = 0.5$ for an ideal chain and 0.6 for a real chain. It is also known that $\nu = 0.588$ for long enough chain in an athermal solvent. In the semi-dilute regime, the

scaling theory predicts the ϕ-dependence of R as

$$R \cong bN^{\nu}\left(\frac{\phi}{\phi^*}\right)^{\frac{2\nu-1}{2(1-3\nu)}} \qquad (\phi^* < \phi_0 < \phi^{**}), \tag{4}$$

where ϕ^{**} is the concentration at which the excluded volume effect is fully screened. Note that Eq. (4) was originally derived for linear chains. For star polymers with large numbers of arms, another scaling regime has been proposed by Daoud[50], but the 4-arm star polymers we used have a small enough number of arms to apply for Eq. (4). In concentrated regime, R is equivalent to the unperturbed dimension:

$$R \cong bN^{1/2} \qquad (\phi^{**} < \phi_0), \tag{5}$$

The description of the elastic modulus in the state of interest (E_{m} at $\phi = \phi_{\mathrm{m}}$) as function of ϕ_0 and ϕ_{m} depends on concentration regimes. Eq. (1), (2), (3), (4) and (5) provide the expression for E_{m} as

$$E_{\mathrm{m}} \sim \phi_0^{\frac{2}{3}}\phi_{\mathrm{m}}^{\frac{1}{3}} \qquad (\phi_0 < \phi^* \text{ and } \phi_{\mathrm{m}} < \phi^*), \tag{6a}$$

$$E_{\mathrm{m}} \sim \phi_0^{\frac{2}{3}}\phi_{\mathrm{m}}^{\frac{9\nu-4}{9\nu-3}} \qquad (\phi_0 < \phi^* \text{and } \phi^* < \phi_{\mathrm{m}} < \phi^{**}), \tag{6b}$$

$$E_{\mathrm{m}} \sim \phi_0^{\frac{2}{3}}\phi_{\mathrm{m}}^{\frac{1}{3}} \qquad (\phi_0 < \phi^* \text{and } \phi^{**} < \phi_{\mathrm{m}} < 1), \tag{6c}$$

$$E_{\mathrm{m}} \sim \phi_0^{\frac{1}{9\nu-3}}\phi_{\mathrm{m}}^{\frac{1}{3}} \qquad (\phi^* < \phi_0 < \phi^{**} \text{ and } \phi_{\mathrm{m}} < \phi^*), \tag{6d}$$

$$E_{\mathrm{m}} \sim \phi_0^{\frac{1}{9\nu-3}} \phi_{\mathrm{m}}^{\frac{9\nu-4}{9\nu-3}} \qquad (\phi^* < \phi_0 < \phi^{**} \text{ and } \phi^* < \phi_{\mathrm{m}} < \phi^{**}), \tag{6e}$$

$$E_{\mathrm{m}} \sim \phi_0^{\frac{1}{9\nu-3}} \phi_{\mathrm{m}}^{\frac{1}{3}} \qquad (\phi^* < \phi_0 < \phi^{**} \text{ and } \phi^{**} < \phi_{\mathrm{m}} < 1), \tag{6f}$$

When a large reduction in gel volume occurs upon deswelling, the conformation of network strands is expected to collapse strongly (i.e., supercoiling), resulting in a considerable deviation from the random coil conformation. Supercoiling becomes pronounced in networks originally prepared in the dilute regime and deswollen to a high concentration. Although this corresponds to Eqs. (6c) and (6f), the random coil conformation is still maintained in the highly deswollen state. Obukhov *et al.* considered that the collapsed conformation of network strands in the highly deswollen state is analogous to the conformation of ring polymers in molten state. Supercoiling becomes pronounced above a certain concentration (ϕ_{c}).[8] They argued that ϕ_{c} is comparable to the concentration where the elastic contribution of chain entanglements becomes dominant, expressed as

$$\phi_{\mathrm{c}} \cong \left(\frac{N_{\mathrm{c}}}{N_{\mathrm{e}}}\right)^{-\frac{1}{\alpha-1}} \tag{7}$$

where N_{c} is the polymerization degree of the network strands, and N_{e} is the

entanglement length in molten state. The exponent α describes the concentration dependence of the plateau modulus (G_0) in polymer solutions ($G_0 \sim \phi^{\alpha}$) ($\alpha = 7/3$ and $9/4$ in θ [51] and good solvent [3], respectively). Here, α is strongly related to the tube diameter and blob size of the entanglement network of polymer.[3, 51] G_0 is the storage elastic modulus that a rubber state polymer has. They introduced the concept of "backbone chain" of a supercoiled strand. The actual supercoiled strand is expected to have jagged conformation. When the strand is coarse-grained, the conformation smoothes out to reveal the "backbone chain." The actual supercoiled strand and its backbone chain obviously overlap with each other, but their radius of gyration differs because their conformation is not exactly the same. They estimated the ϕ_{m}-dependence of polymerization degree (N_{bb}), and the volume fraction (ϕ_{bb}) of the backbone chain on the basis of the conservation of the number of strands ($\phi_{\mathrm{bb}}/N_{\mathrm{bb}} = \phi_{\mathrm{m}}/N_{\mathrm{c}}$). The backbone chain is assumed to obey Gaussian statistics ($R_{\mathrm{bb}} \sim N_{\mathrm{bb}}^{1/2}$). Here, R_{bb} is the end-to-end distance of backbone chain. The ϕ_{m}-dependence of E_{m} for a highly deswollen network whose ϕ_0 is

comparable to ϕ^* is obtained by substituting λR_0 and R_{ref} in Eq. (2) with those of backbone chain:

$$E_{\mathrm{m}} \sim \frac{\phi_{\mathrm{m}}}{N}\left(\frac{\lambda R_0}{R_{\mathrm{ref}}}\right)^2 \sim \frac{\phi_{\mathrm{m}}}{N}\left(\frac{\phi_{\mathrm{m}}}{\phi_0}\right)^{-\frac{2}{3}}\left(\frac{\phi_0^{\frac{2\nu-1}{2(1-3\nu)}}}{\phi_{\mathrm{m}}^{\frac{2\nu-1}{2(1-3\nu)}+\frac{3}{14(1-3\nu)}}}\right)^{-2} \sim \phi_0^{\frac{1}{9\nu-3}}\phi_{\mathrm{m}}^{\frac{19-63\nu}{21(1-3\nu)}}$$

$$(\phi_c < \phi_{\mathrm{m}} < 1), \qquad (8)$$

It should be noted that Eq. (8) gives a much higher exponent for ϕ_{m} than Eqs. (6c) and (6f): $E_{\mathrm{m}} \sim \phi_{\mathrm{m}}^{47/42}$ for typical good solvent systems ($\nu = 0.6$).

Simulation Details

A. Model

We used a coarse-grained model in which the polymer is treated as a string of beads connected by springs. Based on the Kremer-Grest model,[52] all beads interacted via a shifted Lennard-Jones (LJ) 12-6 potential (Eq. (9)). The LJ potential has a minimum at $r_{\mathrm{min}} = 2^{1/6}\sigma$. The cutoff distance r_{cutoff} was set to $2r_{\mathrm{min}}$ to reduce computational time, with constant c such that $U^{\mathrm{LJ}}(r = r_{\mathrm{cutoff}}) = 0$.

$$U^{\mathrm{LJ}} = 4\varepsilon\left[\left(\frac{\sigma}{r}\right)^{12} - \left(\frac{\sigma}{r}\right)^{6}\right] + c, \quad (9)$$

where r is distance between i-th and j-th bead in units of σ and ε is well depth of the potential. Here, σ, ε, and $\tau(\equiv \sigma/\sqrt{\varepsilon})$ are dimensionless physical constants for distance, energy and time, respectively. The beads were connected by the Finitely Extensible Non-linear Elastic potential (FENE) (Eq. (10)).

$$U^{\mathrm{FENE}} = \frac{1}{2}kR_{\max}ln\left[1 - \left(\frac{r}{R_{\max}}\right)^{2}\right], \quad (10)$$

The model parameters are the same as in reference [31]. $R_{\max}$ is the maximum length of nearest-neighboring breads, which was set to $R_{\max} = 1.5$, and k is the spring coefficient of the FENE bond. The motion of beads was driven by Langevin dynamics with a timestep of 0.005τ, non-dimension temperature $T^{*} = 1.0$, and friction $\Gamma = 1.0$.

B. Preparation and production runs

(i) Star polymer solutions

The 4-arm star polymer solutions were simulated using 64 star

polymers each composed of 201 beads in various sizes of simulation cells. The simulation cell is cubic box with volume V. We define the volume fraction of polymers as $\phi \equiv 64 \times 201 \times 4\pi/3\,(\sigma/2)^3/V$. At first, we generated star polymers at nearly the dilute limit ($\phi = 0.0001$) and equilibrated for 1×10^8 MD steps. Then, we decreased the simulation cell isotropically by 1% of volume over 1×10^6 MD steps and then equilibrated for 1×10^8 MD steps at constant volume. By repeating this process we obtained the star polymer solutions with the desired ϕ_0.

(ii) Gels

We prepared two types of star polymers (type A and type B), whose terminal beads can bond only with other terminal beads of the opposite type (Figure 1). We mixed equal amounts of type A and type B (1 : 1). In our system, when the distance between terminal beads is equal to $r_{\min}$ ($= 2^{1/6}\sigma$), a new bond is formed. At various ϕ_0, we simulated the gelation process until all terminal beads reacted, which took up to 2×10^9 MD steps. This process

typically depends on the concentration of the system.

To obtain gel samples at various ϕ_{m}, we varied the simulation cell size after the gelation process. We increased or decreased the simulation cell isotropically by 1% of volume over per 1×10^{6} MD steps and equilibrated for 1×10^{8} MD steps. By repeating this process we obtained gels with the desired ϕ_{m}.

(iii) Uniaxial Stretching Measurement

To measure the equilibrated stress-strain curves, the simulation cell was gradually stretched by changing the aspect ratio of the simulation box. The box was deformed with a constant volume $V = L_x L_y L_{\mathrm{z}} = L_0^3$; $L_x = \lambda L_0$, $L_y = L_z = \lambda^{-1/2} L_0$, where L_0 is the side length of initial cubic simulation cell, and L_x, L_y, and L_z are the size of lengths of the x, y, and z dimensions. We used a constant extension speed (= 1×10^{-8} times / 1 MD step). Nominal stress was calculated from the stress tensor: $s_{\mathrm{N}} = P_{xx} - \left(P_{yy} + P_{zz}\right)/2$, with $P_{\alpha\alpha} = L_0^{-3}\left(\sum_i v_{i,\alpha}\, v_{i,\alpha} + \sum_i r_{i,\alpha}\, f_{\mathrm{b},\alpha}(r_i)\right)$, where $\alpha \in (x, y, z)$. Here, $\boldsymbol{v}_i$ is velocity

of i-th elastic bond, r_i is bond length of i-th elastic bond and $\boldsymbol{f}_{\mathrm{b}}(r_i)$ is force of i-th elastic bond.

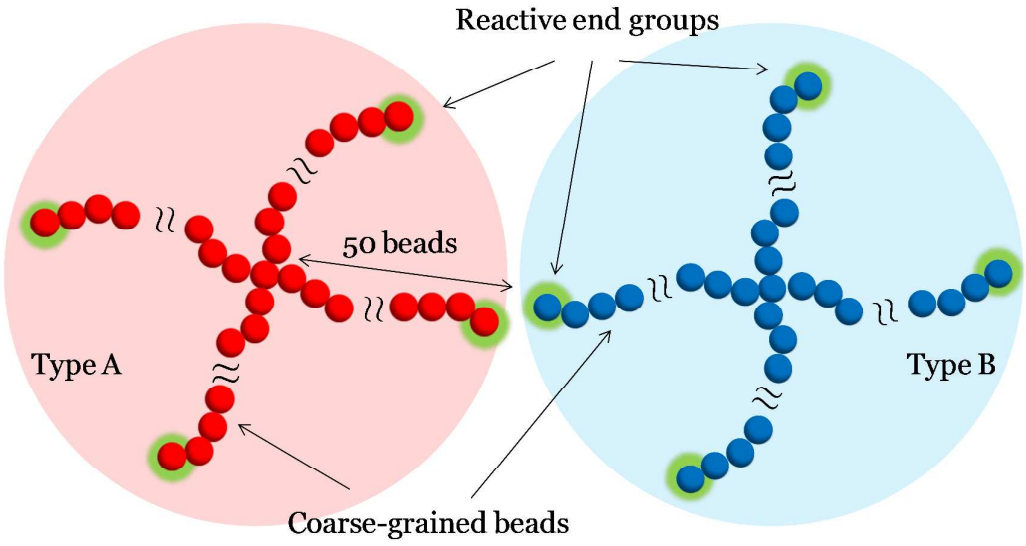

Figure 1. Coarse-grained model of star polymers for Tetra-PEG gels. Spheres represent beads. Red and blue represent type A and type B, respectively. Green represents reactive ends. The ratio of the amount of type A and type B is fixed to 1 : 1. The reactive ends of one type can bond only to the reactive ends of the other type. An arm is composed of 50 beads plus the central bead, so a network strand formed by connecting type A to type B composes 102 beads.

Results and Discussion

I. Verification of the MD simulation

I-1. Radius of gyration of a star polymer and the overlapping concentration

We define the overlapping concentration as

$$\phi^* = \frac{3N_b}{4\pi R_0^3}, \quad (11)$$

where N_b is the number of beads of each star polymer and R_0 is the radius of gyration of star polymers in dilute limit. We investigated the fractal dimension of the star polymers in solution to verify the MD simulation. After enough MD steps for the equilibration, we measured the radius of gyration of the star polymers.

Figure 2 shows the ϕ-dependence of the radius of gyration of the star polymer (R_{star}). To cancel the slight ϕ-dependence of the bond length (b)[32, 53], we compared $\langle R_{star}^2/b^2\rangle/\langle R_0^2/b_0^2\rangle$ with Eq. (4), where b_0 is the bond length in the dilute limit. In the semi-dilute regime we find that our star polymers obey

the same scaling with linear polymers, namely Eq. (4). The intersection point of the scaling $\langle R_{star}^2/b^2\rangle/\langle R_0^2/b_0^2\rangle$ for dilute and semi-dilute regime is approximately located at $\phi/\phi^* \approx 1.0$, implying that Eq. (4) works well to estimate ϕ^* for 4-arm star polymers. These results are in quantitative agreement with a recent study of 4-arm star polymer simulation by Schwenke *et al.*[32] In the high density regime ($\phi > 7.0\ \phi^*$, corresponding to over 23% of polymer volume fraction), the scaling exponent of $\langle R_{\mathrm{star}}^2/b^2\rangle/\langle R_0^2/b_0^2\rangle$ is slightly smaller (≈ -0.3) than the prediction of Eq. (4) with $= 0.6$ (≈ -0.25). This indicates that the gyration of a star polymer is a bit smaller than that of linear polymer at the same degree of polymerization. We interpret this deviation to be caused by the excluded volume effect from the geometric structure of star polymer.

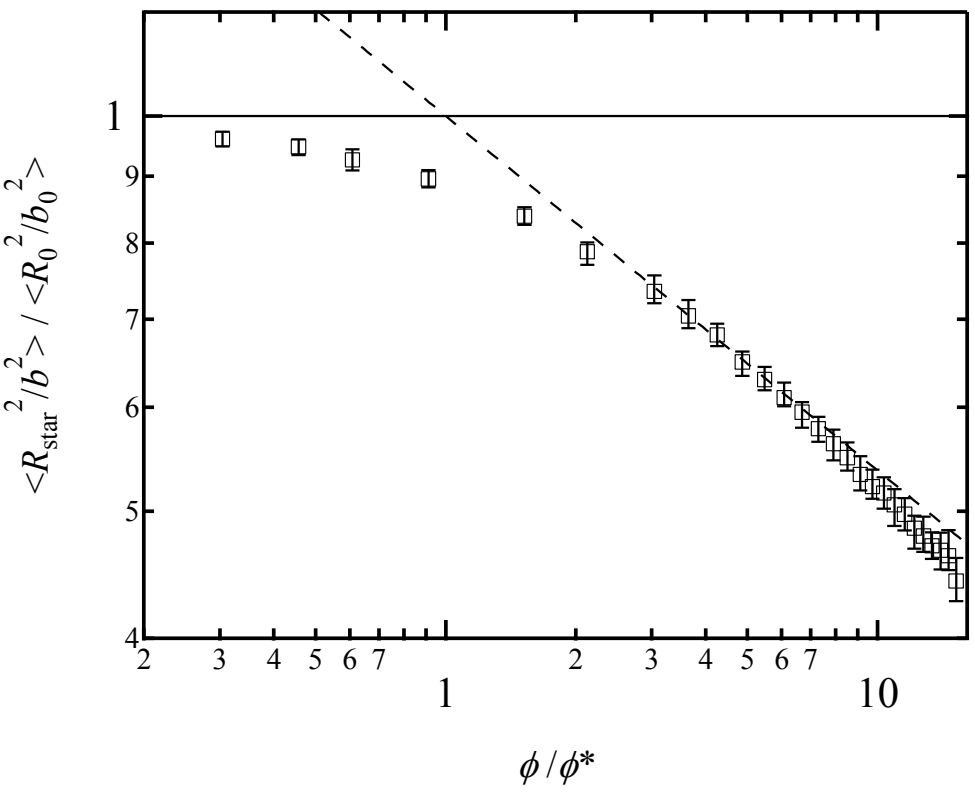

Figure 2. **ϕ-dependence of $\langle R_{star}^2/b^2\rangle/\langle R_0^2/b_0^2\rangle$ of star polymers in solution. Dashed line represent the scaling relationship, $\sim(\phi/\phi^*)^{-0.25}$.**

I-2. Validation of the MD simulation using the elastic modulus

In this section, we discuss the elastic modulus of gels prepared at ϕ_0 and measured at ϕ_m. To measure the equilibriated stress-extension ratio curves, the simulation cell was gradually stretched; the extension speed was

1×10^{-8} times / 1 MD step along the x axis. Nominal stress was calculated from the stress tensor at each deformation ratio. Figure 3 shows examples of stress-elongation ratio curves for as-prepared gels with $\phi_0/\phi^* = 3.0$ and $\phi_0/\phi^* = 6.7$. We determined the Young's modulus from the initial slope of the stress-elongation curves.

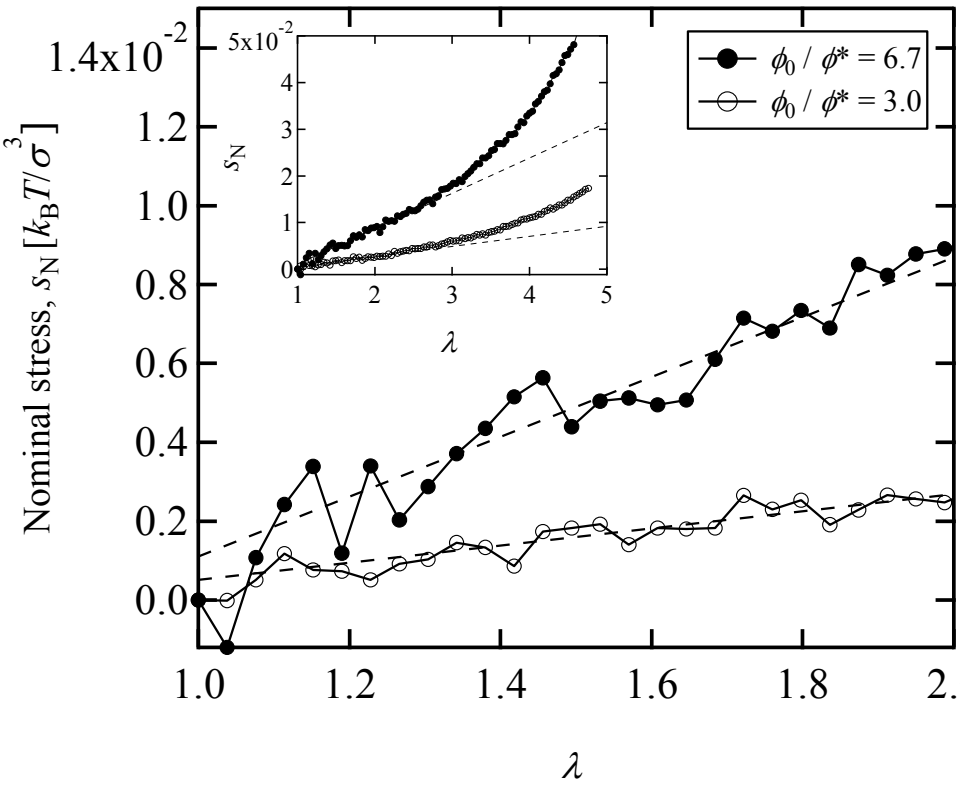

Figure 3. Examples of the stress-elongation ratio relationship for representative gels. Filled and empty circles denote the data for

gels with $\phi_0/\phi^* = 6.7$ and $\phi_0/\phi^* = 3.0$, respectively.

Figure 4 (a) shows simulation results of the ϕ_m-dependence of E_m reduced by the Young's modulus at the preparation state (E_0). We also show our previous experimental results in Figure 4 (b); our experimental data show the power law relationships between E_m and ϕ_m, and exhibit the two crossovers around $\phi/\phi^* \approx 1.0$ and $\phi/\phi^* \approx 4.0$. The slopes in the dilute, semi-dilute and concentrated regimes are 0.33, 0.57 and 1.1, respectively. These slopes and crossovers are well reproduced in our MD simulation (Figure 4 (a)). We can also estimate ϕ_c using Eq. (7). The entanglement length N_e for the bead-spring model has not been unequivocally determined yet, but we can estimate it as roughly $N_e \approx 30$ [54]. Also we have reported that Eq. (7) works to describe the N_c-dependence of ϕ_c, when using the prefactor 0.5 [21]. In the case, using Eq. (7) with $N_c = 102$, $N_e = 30$, $\alpha = 9/4$, and the prefactor 0.5, we get $\phi_c/\phi^* = 5.04$. This estimation is in near quantitative agreement with the $\phi_c/\phi^* \approx 5.0$ we observed in the simulation.

The slopes of 0.33 and 0.56 correspond to the exponents of Eqs. (6a) and (6d), and (6b) and (6e), respectively, in good solvent($\nu = 0.6$). The Obukhov-Rubinstein-Colby model predicts that this crossover occurs at ϕ^*, which corresponds well to both our experimental results and MD simulation. Furthermore, the slope of 1.0 corresponds well to that of Eq. (8), suggesting a supercoiling transformation. Also, in an inset of Figure 4(a), we confirm that the power law relationships between E_m and ϕ_0 for as-prepared gels is $E_\mathrm{m} \sim \phi_0$, which is in good agreement with Eq. (1).

We have confirmed that our MD simulation reproduced experimental results and theoretical predictions. Thus, it is worth investigating the conformation of network strands in MD simulation, which will provide a new insight into the conformational change of network strands caused by macroscopic shrinkage. In the following sections, we analyze the chain conformation at each ϕ_m, and directly compare with the assumptions of the Obukhov-Rubinstein-Colby model.

(a)

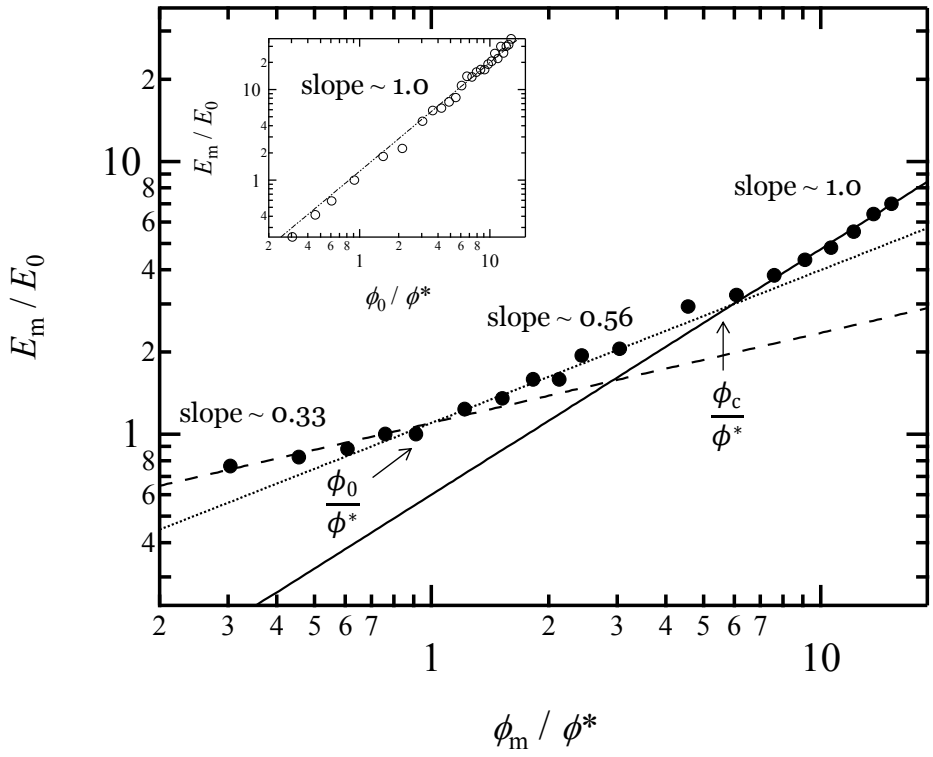

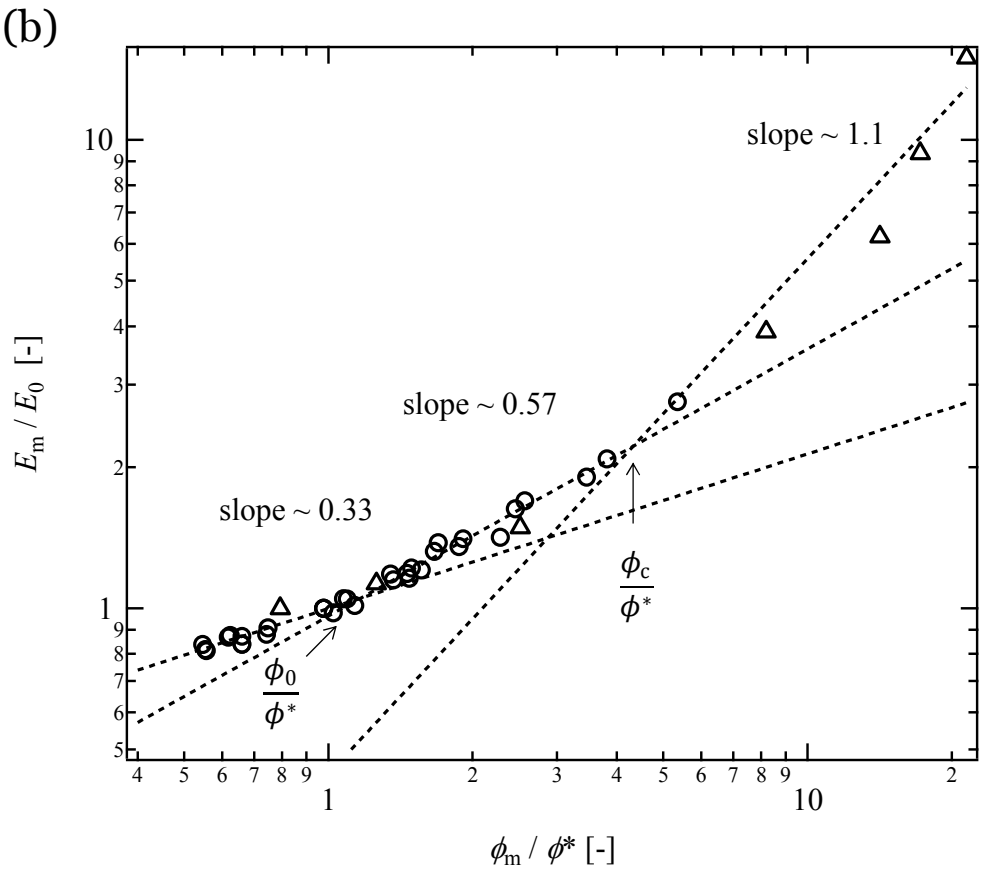

Figure 4. (a) Simulation results of ϕ_m-dependence of E_m for gels prepared at $\phi_0/\phi^* = 0.91$. E_0 is the Young's modulus at $\phi_0/\phi^* = 0.91$. Solid, broken, and dashed lines represent the scaling of E_m for dilute regime, $E_m \sim (\phi_m/\phi^*)^{0.33}$, semi-dilute regime, $E_m \sim (\phi_m/\phi^*)^{0.56}$, and supercoiling regime, $E_m \sim (\phi_m/\phi^*)^{1.0}$, respectively. Inset shows the ϕ_0-dependence of E for gels prepared at various ϕ_0/ϕ^*s. The solid line represents the scaling of $E \sim (\phi_0/\phi^*)^{1.0}$, (b)

Our experimental results. Circles denote data of Tetra-PEG gels with $\phi_0 = 0.034$ and various ϕ_m swollen and deswollen in water.[12] Triangles represent data of Tetra-PEG gels with $\phi_0 = 0.05$ and various ϕ_m in 1-butyl-3-methylimidazolium tetrafluoroborate.[21] Both data are reduced by the Young's modulus E_0 at the preparation state.

II. Verification of the assumptions of the Obukhov-Rubinstein-Colby model

II-1. Conformation of the network strands in dilute and semi-dilute regime

We estimated the averaged end-to-end distance ($\langle R_e^2 \rangle \equiv \frac{1}{N_s}\sum_1^{N_s}|\boldsymbol{v_s}|^2$) and the averaged radius of gyration ($\langle R_g^2 \rangle \equiv \frac{1}{101N_s}\sum_1^{N_s}\sum_1^{101}|\boldsymbol{v_c}|^2$) of all network strands. Here, N_s is the number of network strands, $\boldsymbol{v_s}$ is the vector between ends of a network strand, $\boldsymbol{v_c}$ is the vector between a mass center of a network strand and a bead which composes of the network strand. Figure 5 shows R_e and R_g

against ϕ_m/ϕ^* of the gels formed at $\phi_0/\phi^* = 0.91$. R_e is larger than R_g at the preparation state. R_e decreases with increasing ϕ_m/ϕ^*, and we observe the power law behavior $R_e \sim (\phi_m/\phi^*)^{-0.31}$ for $\phi_m/\phi^* > 2.0$. This result corresponds well to the assumption of the Obukhov-Rubinstein-Colby model that swelling causes crosslinks to move affinely. In contrast, the power law becomes smaller than $1/3$ for $\phi_m/\phi^* < 2.0$. This is because these gels prepared at dilute solution at $\phi_0/\phi^* = 0.91$ have approximately 10% connectivity-defects in the gel.[31, 32, 55] These defects reveal themselves as spatial inhomogeneity in the swollen state,[31] so that we may expect that crosslinks will not move affinely in this case. On the other hand, R_g decreases with increasing ϕ_m/ϕ^* as $R_g \sim (\phi_m/\phi^*)^{-0.125}$ below $\phi_m/\phi^* \approx 2.0$. This behavior corresponds well to the scaling prediction in good solvent,[3] and agrees with the assumption of the Obukhov-Rubinstein-Colby model in semi-dilute regime. Around $\phi_m/\phi^* \approx 2.0$, the ϕ_m-dependence starts to change gradually. Above the onset concentration of supercoiling ($\phi_c/\phi^* \approx 5.0$), R_g deviates from the line at $R_g \sim (\phi_m/\phi^*)^{-0.125}$ and approaches to the scaling of R_e; that is, the

scaling of R_g became $R_g \sim (\phi_m/\phi^*)^{-0.31}$. For reference, we show in Figure 6 the ϕ_m-dependence of R_g/R_e compared to that of as-prepared gels. In as-prepared gels, we find that $R_g/R_e \cong 0.390$ for $\phi_0/\phi^* > 2.0$ and R_g/R_e slightly decreases for $\phi_0/\phi^* < 1.0$. It is well known that $R_g/R_e = \sqrt{1/6} \cong 0.408$ and $R_g/R_e \cong \sqrt{1/6 \times 0.952} \cong 0.393$ for ideal chain and real chain, respectively.[56] The statistic of network strands of as-prepared gels seems to be that of a real chain in the whole region. On the other hand, in swollen/deswollen gels, we clearly find two regimes. $R_g/R_e \sim (\phi_m/\phi^*)^{0.09}$ for $\phi_0/\phi^* < 5.0 \approx \phi_c/\phi^*$ and $R_g/R_e \cong 0.455$ for $\phi_0/\phi^* > 5.0 \approx \phi_c/\phi^*$. In the former regime, this power law of 0.09 is caused by the difference of power law between R_g and R_e as shown in Figure 5. More surprisingly we obtain a very abnormal value ($R_g/R_e \cong 0.455$) in the latter regime. This indicates that the statistics of the network strands becomes abnormal when compared with the statistics of real chains above the onset concentration of supercoiling (ϕ_c/ϕ^*). Note that we interpret that our obtained $R_g/R_e \cong 0.455$ is NOT a universal value for the supercoiling state for two reasons. First, R_g/R_e should be

strongly related to fractal dimension (D_f) of the network strands. Second, D_f of supercoiled network strands likely depends on N_c, as we have already confirmed that D_f increases monotonically with the increase of N_c.[21]

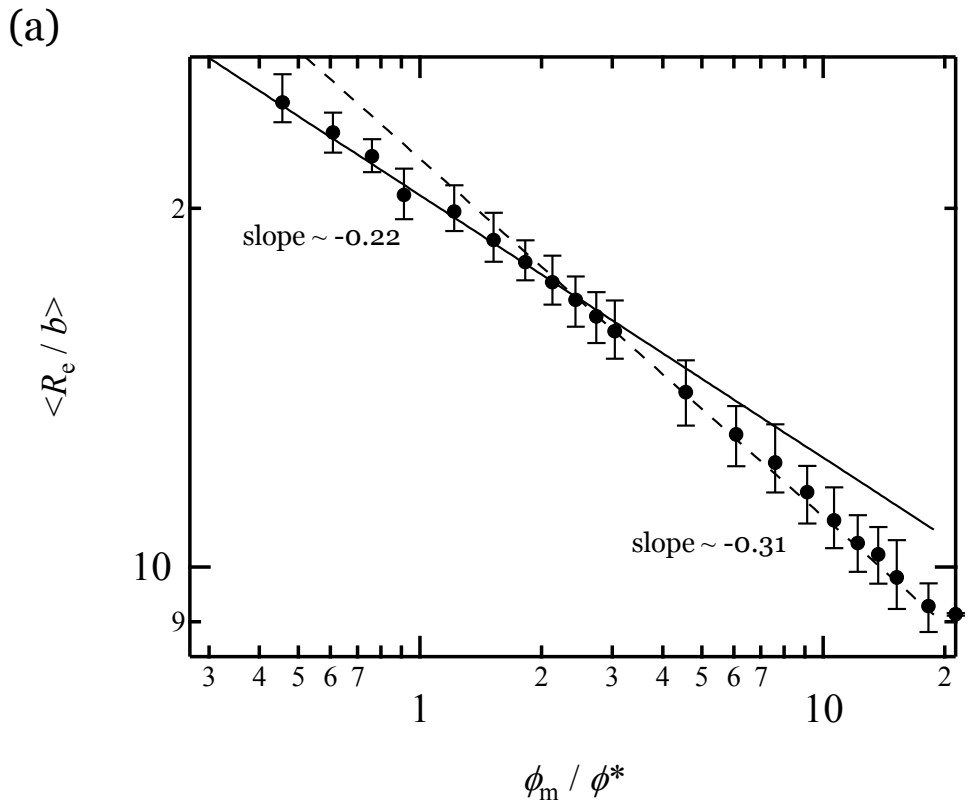

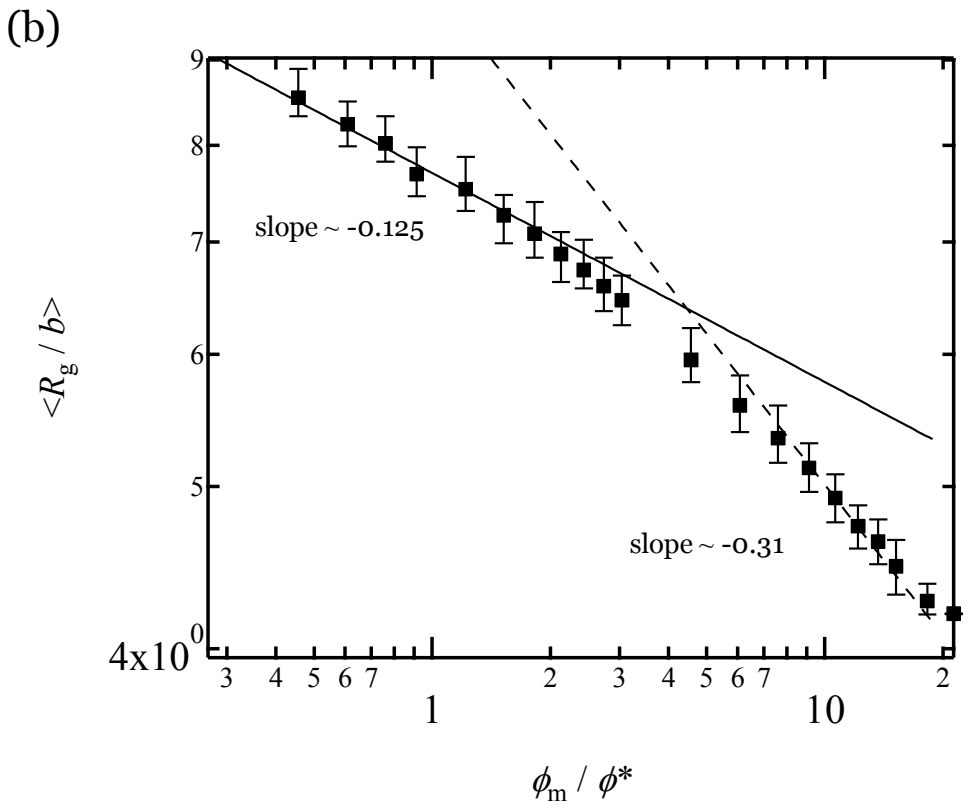

Figure 5. Statistics of the network strands of gels prepared at $\phi_0/\phi^* = 0.91$. (a) ϕ_m-dependence of the end-to-end distance (R_e). Solid line and broken line represent the guide lines for $R_g \sim (\phi_0/\phi^*)^{-0.22}$ and $R_g \sim (\phi_0/\phi^*)^{-0.31}$, respectively. (b) ϕ_m-dependence of the radius of gyration (R_g) Solid line and broken line represent the guide lines for $R_g \sim (\phi_m/\phi^*)^{-0.125}$ and $R_g \sim (\phi_m/\phi^*)^{-0.31}$, respectively.

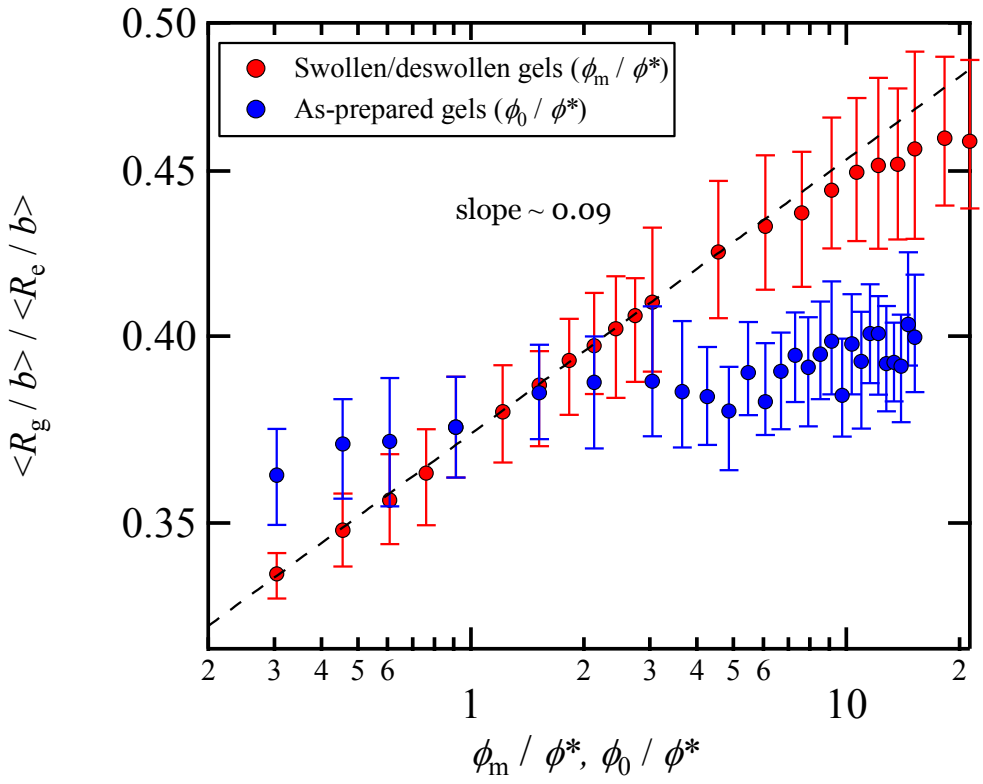

Figure 6. ϕ_0- and ϕ_m-dependence of R_g/R_e.

II-3. Estimation of the fractal dimension of network strands

We discuss here the conformation of the network strands by means of the fractal dimension of network strands (D_f). When a particular network strand has a mass fractal dimension D_f, the relationship between the average number of beads ($\langle N(r) \rangle$) that belongs to the same network strand within the distance r from the center of mass is expressed as

$$\langle N(r)\rangle \sim r^{D_f} \quad (12)$$

Examples of the obtained scaling relationship between $\langle N(r)\rangle$ and r is shown in Figure 7. For each sample, we observed the scaling relationship and estimated D_f from the slope.

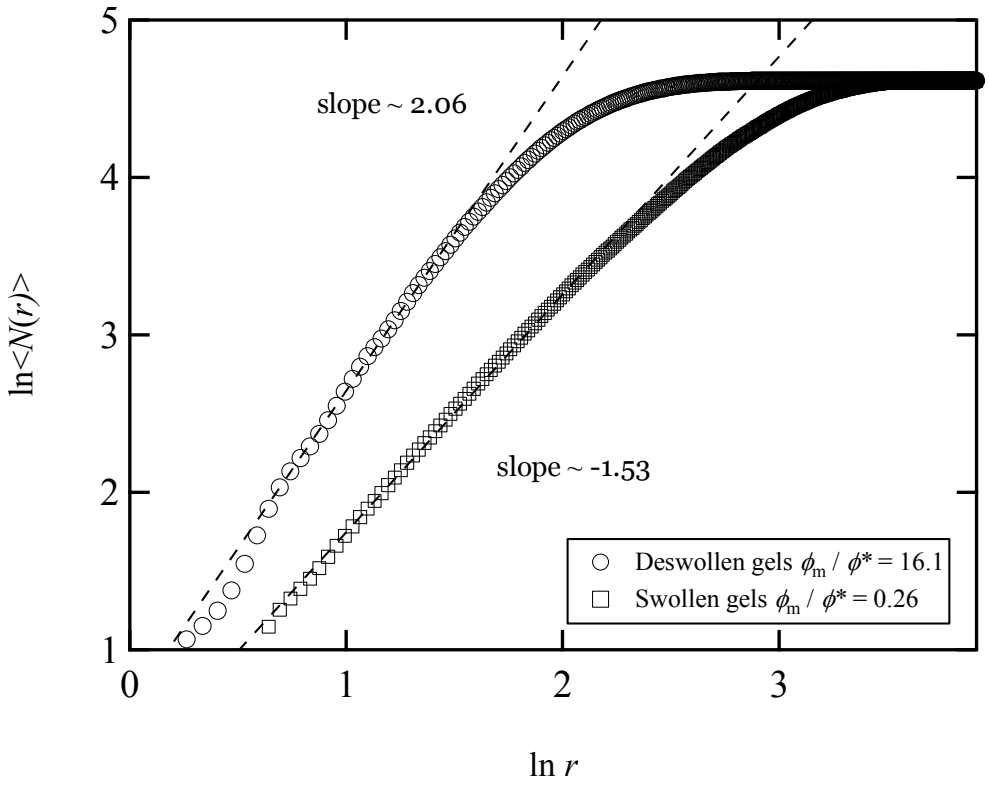

Figure 7. Relationship between the average number of beads ($\langle N(r)\rangle$) within the distance from the center of mass (r) for gels with $\phi_0 = 0.91$. Circles and squares represent gels measured at $\phi_m/\phi^* =$

0.26 and 16.1, respectively.

Figure 8 (a) shows the ϕ_m-dependence of the estimated fractal dimension (D_f) for gels with $\phi_0/\phi^* = 0.91$. As a reference, we compare them with ϕ_0-dependence of D_f for as-prepared gels. In as-prepared gels, D_f is 1.68 at $\phi_0/\phi^* = 0.91$. This corresponds to the theoretical value for real chains. However, D_f becomes 1.62 with a decrease of concentration. This is caused by defects and spatial inhomogeneity. Recent simulation studies[31, 32] and experiments[55] of 4-arm star polymer gels indicate that defects and spatial inhomogeneity drastically increase below ϕ^*. Also D_f reaches 1.77 and becomes constant with further increase of concentration. According to the scaling prediction, this plateau value should be the same with that of an ideal chain. As we indicated in Section I-1, we can presume that star polymers feel additional excluded volume caused by geometric restriction of the star-polymer itself. The deviation of D_f from real chains is caused by this additional excluded volume effect.

On the other hand, D_f increases with increasing ϕ_m and supercoiling becomes pronounced above ϕ_c, where D_f was 2.05. This fractal dimension is very close to that of an ideal chain. However, considering the results of the relationship between the end-to-end distance and the radius of gyration (see Figure 5 and 6), the statistic of the network strands above ϕ_c is quite different from that of an ideal chain.

Figure 8 (b) shows our experimental results on Tetra-PEG gels. In our experiments, we estimated the fractal dimension from stress-elongation curves using a modified Pincus blob concept.[18, 21] The Pincus blob concept originally describes the λ-dependence of σ for a strongly stretched single polymer chain.[33] We modified the model by considering the lateral compression and applying stress-elongation curves in the large deformation regime. The trends of the simulation results corresponds to that of experimental results. The difference in the slope in the lower concentration regime may be attributed to the excluded volume effects. In our experiments, the excluded volume exponent was lower than the simulation (Experiment: 0.56,

Simulation: 0.6). These results suggest that that the Pincus blob approach is valid for the network system.

We show examples of the conformation of the network strands of as-prepared gel with that of deswollen gel at supercoiling regime in Figure 9. It is clearly shown that there is a big difference of R_e between as-prepared gel and supercoiled gel despite that they are at the same concentration. Also in the supercoiled gel, network strands are tightly compact and the conformation looks like a 2-D plane.

(a)

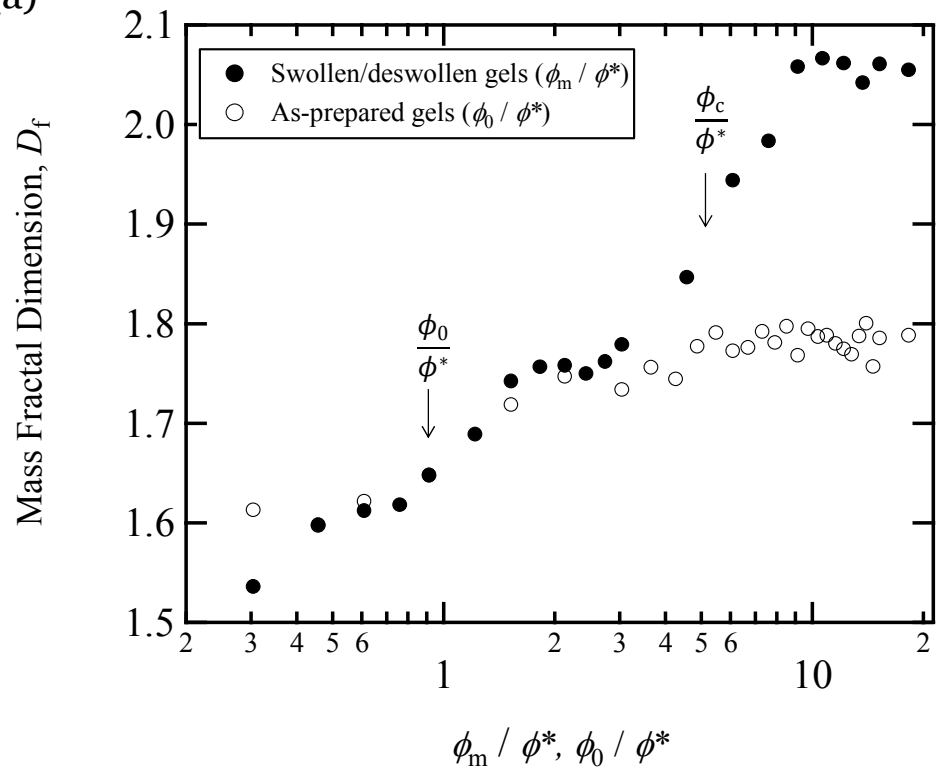

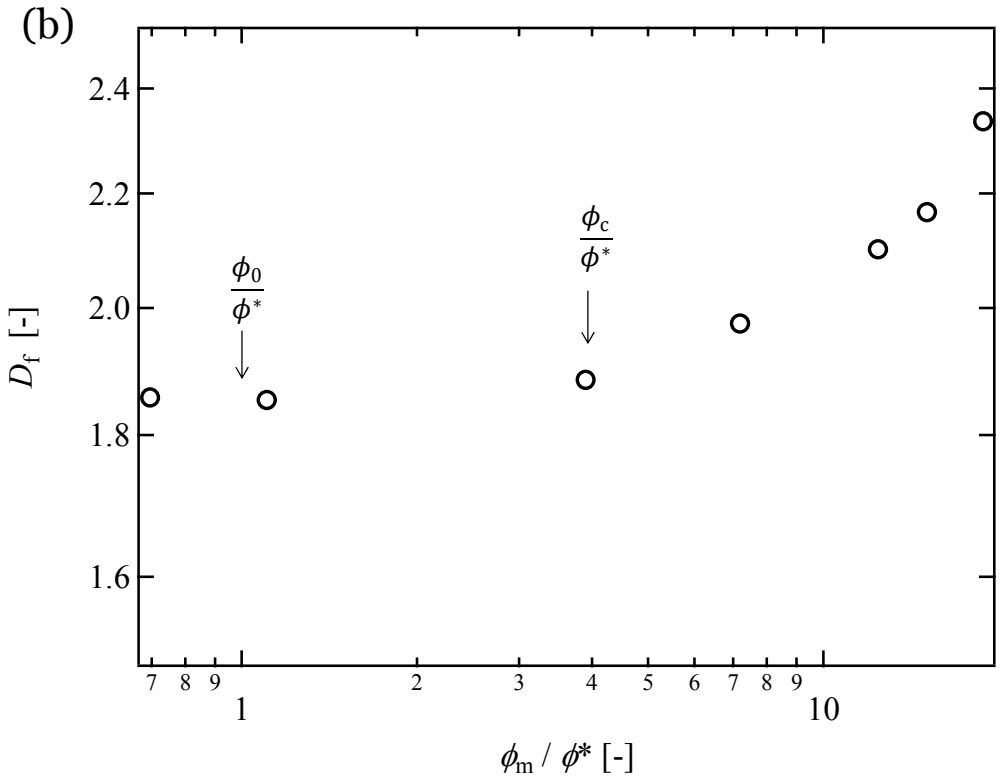

Figure 8. (a) Simulation results of the ϕ_m-dependence of D_f in network strands for gels with $\phi_0 = 0.91$. (b) Our experimental results – Reproduced by permission of the American Institute of Physics.[21] ϕ_c represents the onset concentration of supercoiling.

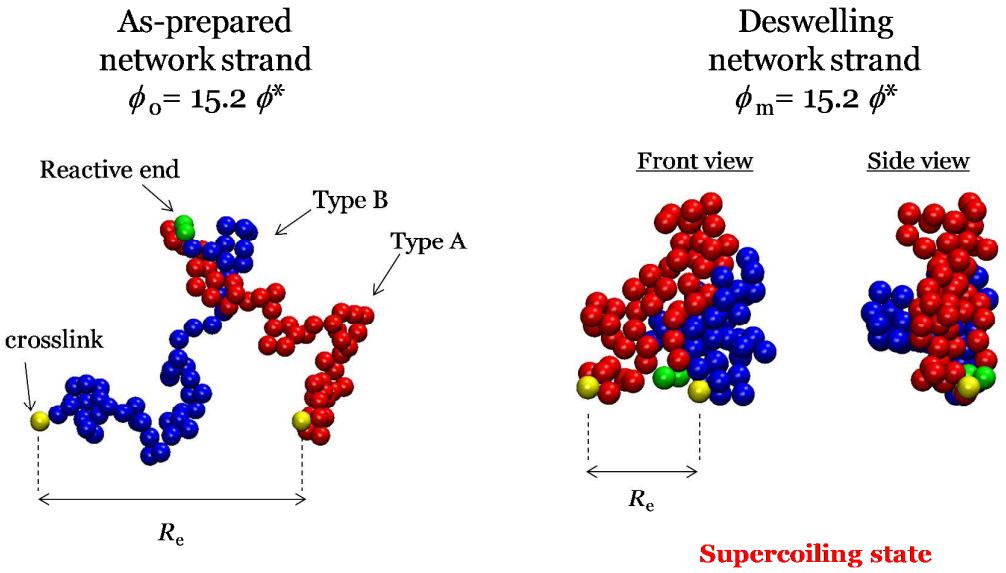

Figure 9. Comparison of confirmation of the network strands of as-prepared gel with that of deswollen gel at same concentration. (a) $\phi_0/\phi^* = 15.2$, $D_f = 1.78$, (b) $\phi_0/\phi^* = 0.91$, $\phi_m/\phi^* = 15.2$, $D_f = 2.06$. Red, blue, green and yellow spheres represent coarse-grained beads of type A, type B, crosslink and reactive end, respectively. Crosslink corresponds to the central bead of a star polymer.

Conclusion

In this study, we used molecular dynamic simulation to directly

observe the effects of swelling and deswelling on the conformation of the network strands and investigated the validity of the Obukhov-Rubinstein-Colby model. We revealed the following points. (1) The MD simulation well reproduces the experimental results of elastic modulus, and this demonstrates its validity. (2) The end-to-end distance of network strands varies affinely during swelling and deswelling. (3) On the other hand, the radius of gyration of network strands obeys the scaling law in good solvent with swelling and deswelling in the dilute and semi-dilute regimes. These behaviors are good agreement with the Obukhov-Rubinstein-Colby model's assumption. When the end-to-end distance decreases due to strong deswelling, the radius of gyration drastically shrinks, which indicates that the strand is "supercoiling." (4) The fractal dimension of supercoiled network strands is much higher than that of an ideal chain, which is in good agreement with experimentally obtained results. We verified for the first time that the Pincus blob approach is valid in terms of molecular interpretation.

Acknowledgements

The authors thank S. K. Kumar, G. S. Grest, and A. Cacciuto for fruitful discussions. We also thank D. Sinkovits and M. Kojima for proofreading our manuscript. This research is supported by the Ministry of Education, Science, Sports and Culture, Japan Grant-in-Aid for Scientific Research, Grant No. 2224518 to MS. We thank the Supercomputer Center, Institute for Solid State Physics, University of Tokyo for the use of its facilities and SGI Altix ICE 8400EX (and/or NEC SX-9). We also thank the Columbia University Information Technology Center for the use of the Yeti HPC cluster system.

Reference

1. J. Bastide, R. Duplessix, C. Picot and S. Candau, *Macromolecules*, 1984, **17**, 83-93.
2. S. Candau, A. Peters and J. Herz, *Polymer*, 1981, **22**, 1504-1510.
3. P. G. de Gennes, *Scaling concepts in polymer physics*, Cornell University Press, Ithaca, N.Y., 1979.
4. P. J. Flory, *Principles of polymer chemistry*, Cornell University Press, Ithaca, 1953.

5. P. J. Flory and J. Rehner, *Journal of Chemical Physics*, 1943, **11**, 521-526.
6. G. Heinrich, E. Straube and G. Helmis, *Advances in Polymer Science*, 1988, **85**, 33-87.
7. R. M. Johnson and J. E. Mark, *Macromolecules*, 1972, **5**, 41-45.
8. S. P. Obukhov, M. Rubinstein and R. H. Colby, *Macromolecules*, 1994, **27**, 3191-3198.
9. C. S. M. Ong and R. S. Stein, *Journal of Polymer Science: Polymer Physics Edition*, 1974, **12**, 1599-1606.
10. S. K. Patel, S. Malone, C. Cohen, J. R. Gillmor and R. H. Colby, *Macromolecules*, 1992, **25**, 5241-5251.
11. C. Price, G. Allen, F. de Candia, M. C. Kirkham and A. Subramaniam, *Polymer*, 1970, **11**, 486-491.
12. T. Sakai, M. Kurakazu, Y. Akagi, M. Shibayama and U.-i. Chung, *Soft Matter*, 2012, **8**, 2730-2736.
13. L. R. G. Treloar, *The physics of rubber elasticity*, Clarendon Press, Oxford :, 1975.
14. K. Urayama, T. Kawamura and S. Kohjiya, *Journal of Chemical Physics*, 1996, **105**, 4833-4840.
15. K. Urayama, T. Kawamura and S. Kohjiya, *Polymer*, 2009, **50**, 347-356.
16. K. Urayama and S. Kohjiya, *Journal of Chemical Physics*, 1996, **104**, 3352-3359.
17. K. Urayama and S. Kohjiya, *Polymer*, 1997, **38**, 955-962.
18. K. Urayama and S. Kohjiya, *European Physical Journal B*, 1998, **2**, 75-78.
19. K. Urayama, K. Yokoyama and S. Kohjiya, *Polymer*, 2000, **41**, 3273-3278.
20. V. G. Vasiliev, L. Z. Rogovina and G. L. Slonimsky, *Polymer*, 1985, **26**, 1667-1676.
21. T. Katashima, M. Asai, K. Urayama, U.-i. Chung and T. Sakai, *The Journal of Chemical Physics*, 2014, **140**, -.
22. P. J. Flory and J. Rehner, *Journal of Chemical Physics*, 1943, **11**, 512-520.
23. T. Sakai, T. Matsunaga, Y. Yamamoto, C. Ito, R. Yoshida, S. Suzuki, N. Sasaki, M. Shibayama and U. I. Chung, *Macromolecules*, 2008, **41**, 5379-5384.
24. Y. Akagi, J. P. Gong, U.-i. Chung and T. Sakai, *Macromolecules*, 2013, **46**, 1035-1040.

25. Y. Akagi, T. Matsunaga, M. Shibayama, U. Chung and T. Sakai, *Macromolecules*, 2010, **43**, 488-493.
26. F. Lange, K. Schwenke, M. Kurakazu, Y. Akagi, U. I. Chung, M. Lane, J. U. Sommer, T. Sakai and K. Saalwachter, *Macromolecules*, 2011, **44**, 9666-9674.
27. T. Matsunaga, T. Sakai, Y. Akagi, U. Chung and M. Shibayama, *Macromolecules*, 2009, **42**, 1344-1351.
28. T. Matsunaga, T. Sakai, Y. Akagi, U. Chung and M. Shibayama, *Macromolecules*, 2009, **42**, 6245-6252.
29. T. Sakai, *Reactive and Functional Polymers*, 2013, **73**, 898-903.
30. T. Sakai, Y. Akagi, T. Matsunaga, M. Kurakazu, U. Chung and M. Shibayama, *Macromolecular Rapid Communications*, 2010, **31**, 1954-1959.
31. M. Asai, T. Katashima, U.-i. Chung, T. Sakai and M. Shibayama, *Macromolecules*, 2013, **46**, 9772-9781.
32. K. Schwenke, M. Lang and J.-U. Sommer, *Macromolecules* 2011, **44**, 9464-9472.
33. P. Pincus, *Macromolecules*, 1976, **9**, 386-388.
34. I. Carmesin and K. Kremer, *Macromolecules*, 1988, **21**, 2819-2823.
35. S. Corezzi, C. De Michele, E. Zaccarelli, D. Fioretto and F. Sciortino, *Soft Matter*, 2008, **4**, 1173-1177.
36. G. S. Grest, B. Dunweg and K. Kremer, *Comput. Phys. Commun.*, 1989, **55**, 269-285.
37. G. S. Grest and K. Kremer, *Macromolecules*, 1990, **23**, 4994-5000.
38. G. S. Grest, M. Putz, R. Everaers and K. Kremer, *Journal of Non-Crystalline Solids*, 2000, **274**, 139-146.
39. J. D. Halverson, W. B. Lee, G. S. Grest, A. Y. Grosberg and K. Kremer, *J Chem Phys*, 2011, **134**, 13.
40. M. Lang, D. Göritz and S. Kreitmeier, *Macromolecules*, 2003, **36**, 4646-4658.
41. M. Lang, D. Göritz and S. Kreitmeier, *Macromolecules*, 2005, **38**, 2515-2523.
42. K. J. Lee and B. E. Eichinger, *Macromolecules*, 1989, **22**, 1441-1448.
43. Y. K. Leung and B. E. Eichinger, *The Journal of Chemical Physics*, 1984, **80**, 3877-3884.
44. M. Murat and G. S. Grest, *Macromolecules*, 1996, **29**, 1278-1285.
45. S. Plimpton, *Journal of Computational Physics*, 1995, **117**, 1-19.

46. K. Schwenke, M. Lang and J. U. Sommer, *Macromolecules*, 2011, **44**, 9464-9472.
47. L. Y. Shy and B. E. Eichinger, *Macromolecules*, 1986, **19**, 2787-2793.
48. H. L. Trautenberg, J.-U. Sommer and D. Göritz, *Macromolecular Symposia*, 1994, **81**, 153-160.
49. S. V. Panyukov, *Zh. Eksp. Teor. Fiz.*, 1990, **98**, 668-680.
50. M. Daoud and J. P. Cotton, *Journal De Physique*, 1982, **43**, 531-538.
51. R. H. Colby and M. Rubinstein, *Macromolecules*, 1990, **23**, 2753-2757.
52. K. Kremer and G. S. Grest, *The Journal of Chemical Physics*, 1990, **92**, 5057-5086.
53. W. Paul, K. Binder, D. W. Heermann and K. Kremer, *J. Phys. II Fr.*, 1991, **1**, 37-60.
54. M. Putz, K. Kremer and G. Grest, *EUROPHYSICS LETTERS*, 2000, **49**, 735-741.
55. F. Lange, K. Schwenke, M. Kurakazu, Y. Akagi, U. Chung, M. Lang, J.-U. Sommer, T. Sakai and K. Saalwaechter, *Macromolecules*, 2011, **44**, 9666–9674.
56. M. Doi and S. F. Edwards, *The Theory of Polymer Dynamics*, Oxford Univ. Press, Oxford, 1986.